

Supplemental File For: Circulating tumor DNA sequencing of gastroesophageal adenocarcinoma.

Supplemental Legend:

Supplemental Table S1. Description of cohorts and sub-cohorts utilized in this study.

Supplemental Table S2. Clinical information detailing patients in the “Baseline-cohort” ie untreated stage IV patients from UC and SMC who underwent ctDNA-NGS testing (n=144).

Supplemental Table S3. Peri-operative ctDNA samples and their timing relative to surgery, DFS, maxVAF at the time of draw, and staging.

Supplemental Table S4. Alterations detected in ctDNA in post-operative patients within 180 days of surgery.

Supplemental Table S5. Frequencies of **A)** genomic alterations, **B)** mutations, or **C)** amplifications in initial tests across the entire Global GEA (n=1627) and UC/SMC subsets as seen in Figure 3. **D)** GA frequencies in genes common to ctDNA-NGS, MSK-Impact, and TCGA reported as percentage altered.

Supplemental Table S6. Frequencies of GAs across the “Global-cohort” and UC/SMC subsets when narrowing patients from figure 3A to **A)** only initial tests with detectable non-synonymous alterations (n=1329) or **B)** only initial tests with maxVAF>0.5% (n=936), as seen in figure S3A-B. Similarly, initial tests from the “Global-cohort” were compared with MSK-Impact and TCGA using **C)** only ctDNA-NGS cases with non-synonymous alterations and **D)** ctDNA-NGS cases with maxVAF>0.5%.

Supplemental Table S7. Detailed molecular information regarding clinically *HER2*-positive patient cohort (n=58).

Supplemental Table S8. Alterations present upon progression of disease after 1L *HER2*-targeted therapy in patients with persistent *HER2* amplification.

Supplemental Table S9. Prognostic significance of alterations, mutations, and amplifications in potentially actionable genes.

Supplemental Figure S1. Relationship between tumor burden, number of alterations, and tumor mutation burden.

A) Amongst untreated stage IV GEA patients, the number of alterations detected (including synonymous) was directly related to the maxVAF (i.e. quantity of ctDNA). **B)** Calculated ctDNA tumor mutation burden correlated with the overall number of alterations detected and **C)** number of mutations detected (by excluding copy number alterations), as expected. **D)** When comparing TMB estimation by ctDNA-NGS with tissue-NGS, no clear correlation is evident. **E)** TMB correction by ctDNA-NGS and **F)** TMB correction by tissue-NGS One were both independent of maxVAF, unlike the number of alterations detected.

Supplemental Figure S2. Number of detected genomic alterations by stage.

Distribution of genomic alterations (excluding synonymous mutations) per initial test by stage (black = mean, red = median) demonstrating that patients with stage IV disease have a trend towards higher number of alterations. Density represents the fraction of patients with a given number of GAs **A)** Stage I (n=9, mean=1.3, median 1) **B)** Stage II (n=22, mean=3.2, median 3) **C)** Stage III (n=59, mean=2.2, median 2) **D)** Stage IV (n=279, mean=4.2, median 3).

Supplemental Figure S3. Relative frequency of common (>5%) non-synonymous alterations between various ctDNA-NGS and tissue-NGS cohorts amongst patients with detectable alterations.

Analyses from Figure 3A and 3D were reproduced using the subsets of patients only with ctDNA alterations present and/or having a maxVAF of at least 0.5%; genes with alteration frequencies >5% are shown. **A)** Comparing incidences between the global versus UC and SMC cohort patients highlights that alteration frequencies equalized between UC and SMC when removing low-shedding ctDNA patients from the analysis. **B)** Similar results were seen when further filtered to patients with a maxVAF >0.5%. **C)** When comparing ctDNA-NGS with MSK-Impact and TCGA after filtering out non-altered ctDNA cases, alterations in EGFR and MET were still notably more common in ctDNA **D)** Differences seen in *TP53* mutation rate are no longer significant one patients are limited to those with maxVAF >0.5% - likely due to elimination of low-shedders, whereas lower *HER2* amplification in ctDNA remains significant, which presumably results from amplification loss after *HER2*-targeted therapy.

Supplemental Figure S4. Distribution of oncogenic copy number with and without “adjustment” for maxVAF.

A) The density distribution of amplifications in clinically relevant genes from 554 tests with insert image showing the lower density range, demonstrating predominantly low-level amplifications in *EGFR* and *MET*. B) Adjusted copy was obtained by normalizing copy number versus maxVAF, which further highlighted the predominantly low-level amplification of *MET* versus more pronounced tails for *FGFR2* and *HER2*.

Supplemental Figure S5.

Serial NGS of ctDNA and tissue highlight spatio-temporal heterogeneity in patients with RTK alterations treated with matched targeted therapies. **A) Patient 1:** Image indicating the presence or absence of *EGFR* and *FGFR2* amplifications over treatment course, analyzed by NGS in various tissue compartments (primary, colon, ascites, ctDNA) as well as FISH confirmatory analyses. *EGFR* amplification was present prior to treatment in the primary tumor and ctDNA, then eradicated in all compartments upon EGFR-targeting. **B) Patient 1:** Plot of *FGFR2* (red) and *EGFR* (green) amplifications over time, analyzed by NGS copy number and FISH ratios (*EGFR/CEN7*; *FGFR2/CEP10*). *FGFR2* amplification increased rapidly when the patient was on *EGFRi* + FOLFOX and FOLFIRI, but decreased to zero once *FGFR2i* was added. **C) Patient 2:** Image indicating the presence or absence of *HER2* amplification throughout time, analyzed by FISH, NGS, and Mass Spectrometry (MS) in various compartments (primary, liver, ctDNA). **D) Patient 2:** Plot of *HER2* amplification by FISH (green) and NGS (red) over time. Copy number is highly amplified at baseline, but decreases in both primary tissue and ctDNA when the patient is on *HER2i*. When the patient is taken off *HER2i*, its amplification level resurges. **E) Patient 3:** Image indicating the presence or absence of *MET* and *KRAS* amplifications throughout time, analyzed by NGS and MS in various compartments (primary, adrenal, ctDNA). **F) Patient 3:** Plot of *MET/KRAS* amplifications and *PIK3CA* mutation in the blood over time. While on MET inhibition and clearance of *MET* amplification in the blood, there is expansion of *KRAS* amplification and acquisition of a new *PIK3CA* mutation. **G) Patient 4:** Image indicating the presence or absence of PD-L1, *MYC/FGFR2/FGFR1* amplifications mutation in various compartments (primary, lymph node, liver, ctDNA) throughout time. **H) Patient 4:** Plot of *MYC* (red), *FGFR2* (green), and *FGFR1* (blue) amplifications over time using copy number. *FGFR2* amplification peaks at recurrence, at which time the patient is put on an *FGFR2* inhibitor, and *FGFR2* amplification subsequently decreased. The expansion in *MYC* and *FGFR1* amplification was observed at progression. **I) Patient 5:** Image indicating the presence or absence of *FGFR2* and *HER2* amplifications throughout time, analyzed by NGS and FISH in various compartments (primary, lymph node, ctDNA). **J) Patient 5:** Plot of *HER2/FGFR2* ctDNA amplifications and *ARID1A/PIK3CA* mutations in the blood over time. With resurgence of *FGFR2*, there is expansion of *ARID1A* mutation and acquisition of a new *PIK3CA* mutation.

Figure S1

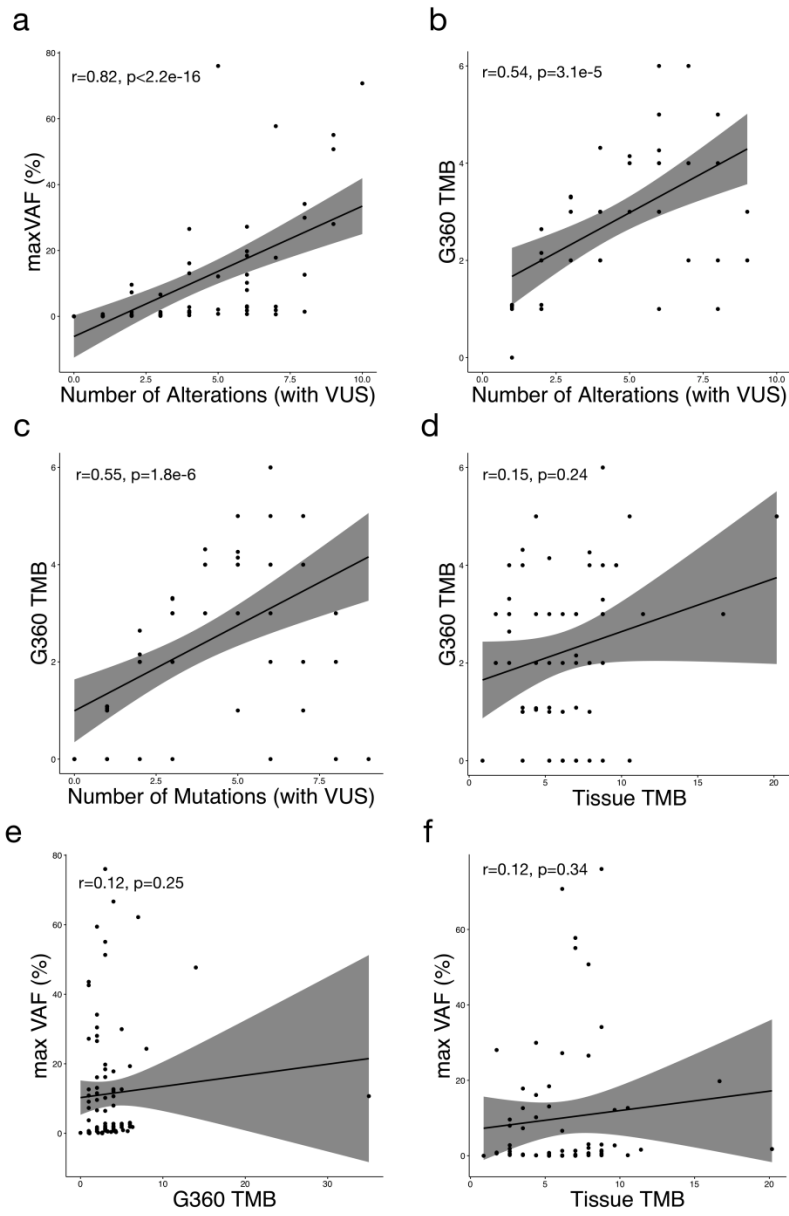


Figure S2

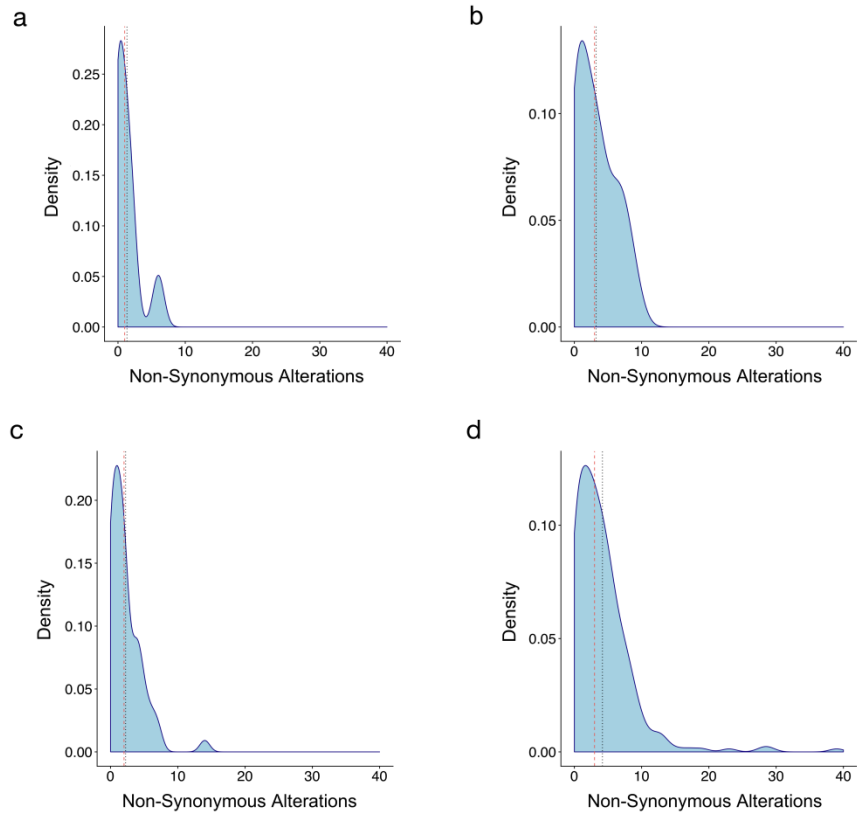
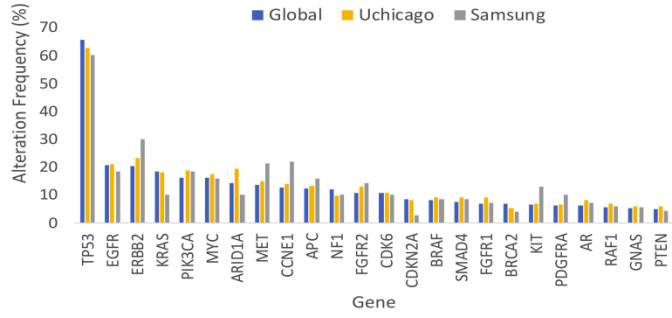
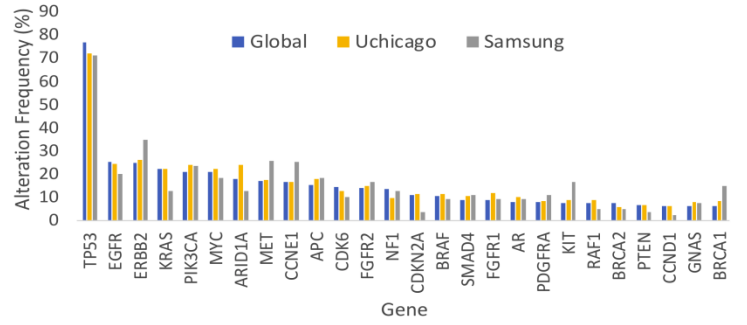


Figure S3

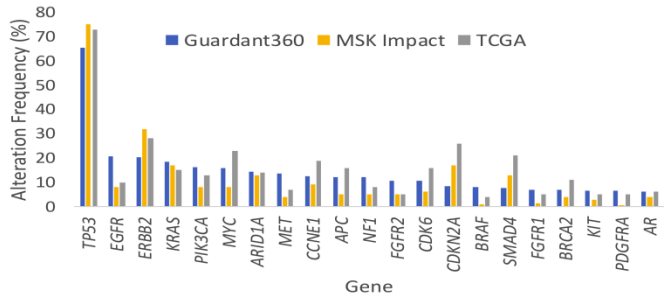
a



b



c



d

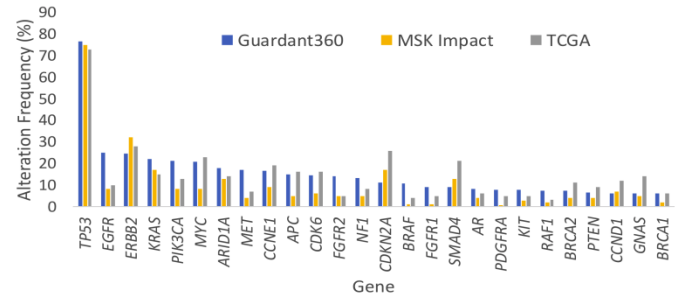


Figure S4

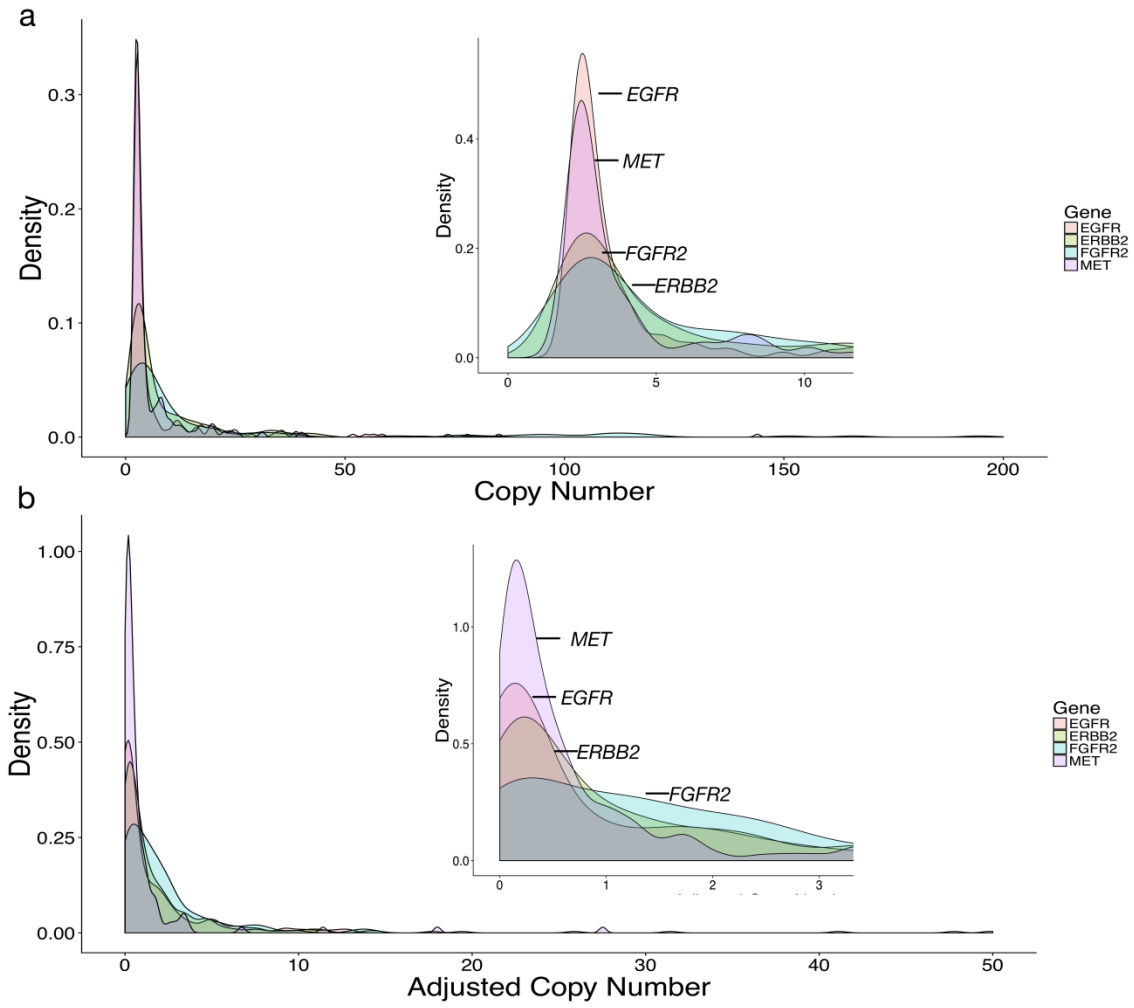


Figure S5

